

Study of the Lepton Flavor Violating Decay $\tau^- \rightarrow \mu^- \eta$

The *BABAR* Collaboration

February 4, 2019

Abstract

We present the preliminary results from the search of the non-conservation of lepton flavor number in the decay of a τ to a lighter mass lepton and a pseudo-scalar meson, performed using $e^+e^- \rightarrow \tau^+\tau^-$ events collected at a center-of-mass energy near 10.58 GeV with the *BABAR* detector at the SLAC PEP-II e^+e^- storage ring. No evidence of such a signal has been found in the data sample corresponding to a luminosity of 314.5 fb^{-1} , and we set an upper limit of 1.6×10^{-7} at 90% confidence level on the decay of $\tau^- \rightarrow \mu^- \eta$.

Submitted to the 33rd International Conference on High-Energy Physics, ICHEP 06,
26 July—2 August 2006, Moscow, Russia.

Stanford Linear Accelerator Center, Stanford University, Stanford, CA 94309

Work supported in part by Department of Energy contract DE-AC03-76SF00515.

The BABAR Collaboration,

B. Aubert, R. Barate, M. Bona, D. Boutigny, F. Couderc, Y. Karyotakis, J. P. Lees, V. Poireau,
V. Tisserand, A. Zghiche

*Laboratoire de Physique des Particules, IN2P3/CNRS et Université de Savoie, F-74941 Annecy-Le-Vieux,
France*

E. Grauges

Universitat de Barcelona, Facultat de Física, Departament ECM, E-08028 Barcelona, Spain

A. Palano

Università di Bari, Dipartimento di Fisica and INFN, I-70126 Bari, Italy

J. C. Chen, N. D. Qi, G. Rong, P. Wang, Y. S. Zhu

Institute of High Energy Physics, Beijing 100039, China

G. Eigen, I. Ofte, B. Stugu

University of Bergen, Institute of Physics, N-5007 Bergen, Norway

G. S. Abrams, M. Battaglia, D. N. Brown, J. Button-Shafer, R. N. Cahn, E. Charles, M. S. Gill,
Y. Groysman, R. G. Jacobsen, J. A. Kadyk, L. T. Kerth, Yu. G. Kolomensky, G. Kukartsev, G. Lynch,
L. M. Mir, T. J. Orimoto, M. Pripstein, N. A. Roe, M. T. Ronan, W. A. Wenzel

Lawrence Berkeley National Laboratory and University of California, Berkeley, California 94720, USA

P. del Amo Sanchez, M. Barrett, K. E. Ford, A. J. Hart, T. J. Harrison, C. M. Hawkes, S. E. Morgan,
A. T. Watson

University of Birmingham, Birmingham, B15 2TT, United Kingdom

T. Held, H. Koch, B. Lewandowski, M. Pelizaeus, K. Peters, T. Schroeder, M. Steinke
Ruhr Universität Bochum, Institut für Experimentalphysik 1, D-44780 Bochum, Germany

J. T. Boyd, J. P. Burke, W. N. Cottingham, D. Walker

University of Bristol, Bristol BS8 1TL, United Kingdom

D. J. Asgeirsson, T. Cuhadar-Donszelmann, B. G. Fulsom, C. Hearty, N. S. Knecht, T. S. Mattison,
J. A. McKenna

University of British Columbia, Vancouver, British Columbia, Canada V6T 1Z1

A. Khan, P. Kyberd, M. Saleem, D. J. Sherwood, L. Teodorescu

Brunel University, Uxbridge, Middlesex UB8 3PH, United Kingdom

V. E. Blinov, A. D. Bukin, V. P. Druzhinin, V. B. Golubev, A. P. Onuchin, S. I. Serednyakov,
Yu. I. Skovpen, E. P. Solodov, K. Yu Todyshev

Budker Institute of Nuclear Physics, Novosibirsk 630090, Russia

D. S. Best, M. Bondioli, M. Bruinsma, M. Chao, S. Curry, I. Eschrich, D. Kirkby, A. J. Lankford, P. Lund,
M. Mandelkern, R. K. Mommsen, W. Roethel, D. P. Stoker

University of California at Irvine, Irvine, California 92697, USA

S. Abachi, C. Buchanan

University of California at Los Angeles, Los Angeles, California 90024, USA

S. D. Foulkes, J. W. Gary, O. Long, B. C. Shen, K. Wang, L. Zhang
University of California at Riverside, Riverside, California 92521, USA

H. K. Hadavand, E. J. Hill, H. P. Paar, S. Rahatlou, V. Sharma
University of California at San Diego, La Jolla, California 92093, USA

J. W. Berryhill, C. Campagnari, A. Cunha, B. Dahmes, T. M. Hong, D. Kovalskyi, J. D. Richman
University of California at Santa Barbara, Santa Barbara, California 93106, USA

T. W. Beck, A. M. Eisner, C. J. Flacco, C. A. Heusch, J. Kroseberg, W. S. Lockman, G. Nesom, T. Schalk,
B. A. Schumm, A. Seiden, P. Spradlin, D. C. Williams, M. G. Wilson
University of California at Santa Cruz, Institute for Particle Physics, Santa Cruz, California 95064, USA

J. Albert, E. Chen, A. Dvoretzkii, F. Fang, D. G. Hitlin, I. Narsky, T. Piatenko, F. C. Porter, A. Ryd,
A. Samuel
California Institute of Technology, Pasadena, California 91125, USA

G. Mancinelli, B. T. Meadows, K. Mishra, M. D. Sokoloff
University of Cincinnati, Cincinnati, Ohio 45221, USA

F. Blanc, P. C. Bloom, S. Chen, W. T. Ford, J. F. Hirschauer, A. Kreisel, M. Nagel, U. Nauenberg,
A. Olivas, W. O. Ruddick, J. G. Smith, K. A. Ulmer, S. R. Wagner, J. Zhang
University of Colorado, Boulder, Colorado 80309, USA

A. Chen, E. A. Eckhart, A. Soffer, W. H. Toki, R. J. Wilson, F. Winklmeier, Q. Zeng
Colorado State University, Fort Collins, Colorado 80523, USA

D. D. Altenburg, E. Feltresi, A. Hauke, H. Jasper, J. Merkel, A. Petzold, B. Spaan
Universität Dortmund, Institut für Physik, D-44221 Dortmund, Germany

T. Brandt, V. Klose, H. M. Lacker, W. F. Mader, R. Nogowski, J. Schubert, K. R. Schubert, R. Schwierz,
J. E. Sundermann, A. Volk
Technische Universität Dresden, Institut für Kern- und Teilchenphysik, D-01062 Dresden, Germany

D. Bernard, G. R. Bonneaud, E. Latour, Ch. Thiebaux, M. Verderi
Laboratoire Leprince-Ringuet, CNRS/IN2P3, Ecole Polytechnique, F-91128 Palaiseau, France

P. J. Clark, W. Gradl, F. Muheim, S. Playfer, A. I. Robertson, Y. Xie
University of Edinburgh, Edinburgh EH9 3JZ, United Kingdom

M. Andreotti, D. Bettoni, C. Bozzi, R. Calabrese, G. Cibinetto, E. Luppi, M. Negrini, A. Petrella,
L. Piemontese, E. Prencipe
Università di Ferrara, Dipartimento di Fisica and INFN, I-44100 Ferrara, Italy

F. Anulli, R. Baldini-Ferrolì, A. Calcaterra, R. de Sangro, G. Finocchiaro, S. Pacetti, P. Patteri,
I. M. Peruzzi,¹ M. Piccolo, M. Rama, A. Zallo
Laboratori Nazionali di Frascati dell'INFN, I-00044 Frascati, Italy

¹Also with Università di Perugia, Dipartimento di Fisica, Perugia, Italy

A. Buzzo, R. Capra, R. Contri, M. Lo Vetere, M. M. Macri, M. R. Monge, S. Passaggio, C. Patrignani,
E. Robutti, A. Santroni, S. Tosi

Università di Genova, Dipartimento di Fisica and INFN, I-16146 Genova, Italy

G. Brandenburg, K. S. Chaisanguanthum, M. Morii, J. Wu

Harvard University, Cambridge, Massachusetts 02138, USA

R. S. Dubitzky, J. Marks, S. Schenk, U. Uwer

Universität Heidelberg, Physikalisches Institut, Philosophenweg 12, D-69120 Heidelberg, Germany

D. J. Bard, W. Bhimji, D. A. Bowerman, P. D. Dauncey, U. Egede, R. L. Flack, J. A. Nash,
M. B. Nikolich, W. Panduro Vazquez

Imperial College London, London, SW7 2AZ, United Kingdom

P. K. Behera, X. Chai, M. J. Charles, U. Mallik, N. T. Meyer, V. Ziegler

University of Iowa, Iowa City, Iowa 52242, USA

J. Cochran, H. B. Crawley, L. Dong, V. Eyges, W. T. Meyer, S. Prell, E. I. Rosenberg, A. E. Rubin

Iowa State University, Ames, Iowa 50011-3160, USA

A. V. Gritsan

Johns Hopkins University, Baltimore, Maryland 21218, USA

A. G. Denig, M. Fritsch, G. Schott

Universität Karlsruhe, Institut für Experimentelle Kernphysik, D-76021 Karlsruhe, Germany

N. Arnaud, M. Davier, G. Grosdidier, A. Höcker, F. Le Diberder, V. Lepeltier, A. M. Lutz, A. Oyanguren,
S. Pruvot, S. Rodier, P. Roudeau, M. H. Schune, A. Stocchi, W. F. Wang, G. Wormser

*Laboratoire de l'Accélérateur Linéaire, IN2P3/CNRS et Université Paris-Sud 11, Centre Scientifique
d'Orsay, B.P. 34, F-91898 ORSAY Cedex, France*

C. H. Cheng, D. J. Lange, D. M. Wright

Lawrence Livermore National Laboratory, Livermore, California 94550, USA

C. A. Chavez, I. J. Forster, J. R. Fry, E. Gabathuler, R. Gamet, K. A. George, D. E. Hutchcroft,
D. J. Payne, K. C. Schofield, C. Touramanis

University of Liverpool, Liverpool L69 7ZE, United Kingdom

A. J. Bevan, F. Di Lodovico, W. Menges, R. Sacco

Queen Mary, University of London, E1 4NS, United Kingdom

G. Cowan, H. U. Flaecher, D. A. Hopkins, P. S. Jackson, T. R. McMahon, S. Ricciardi, F. Salvatore,
A. C. Wren

*University of London, Royal Holloway and Bedford New College, Egham, Surrey TW20 0EX, United
Kingdom*

D. N. Brown, C. L. Davis

University of Louisville, Louisville, Kentucky 40292, USA

J. Allison, N. R. Barlow, R. J. Barlow, Y. M. Chia, C. L. Edgar, G. D. Lafferty, M. T. Naisbit,
J. C. Williams, J. I. Yi

University of Manchester, Manchester M13 9PL, United Kingdom

C. Chen, W. D. Hulsbergen, A. Jawahery, C. K. Lae, D. A. Roberts, G. Simi

University of Maryland, College Park, Maryland 20742, USA

G. Blaylock, C. Dallapiccola, S. S. Hertzbach, X. Li, T. B. Moore, S. Saremi, H. Staengle

University of Massachusetts, Amherst, Massachusetts 01003, USA

R. Cowan, G. Sciolla, S. J. Sekula, M. Spitznagel, F. Taylor, R. K. Yamamoto

*Massachusetts Institute of Technology, Laboratory for Nuclear Science, Cambridge, Massachusetts 02139,
USA*

H. Kim, S. E. McLachlin, P. M. Patel, S. H. Robertson

McGill University, Montréal, Québec, Canada H3A 2T8

A. Lazzaro, V. Lombardo, F. Palombo

Università di Milano, Dipartimento di Fisica and INFN, I-20133 Milano, Italy

J. M. Bauer, L. Cremaldi, V. Eschenburg, R. Godang, R. Kroeger, D. A. Sanders, D. J. Summers,
H. W. Zhao

University of Mississippi, University, Mississippi 38677, USA

S. Brunet, D. Côté, M. Simard, P. Taras, F. B. Viaud

Université de Montréal, Physique des Particules, Montréal, Québec, Canada H3C 3J7

H. Nicholson

Mount Holyoke College, South Hadley, Massachusetts 01075, USA

N. Cavallo,² G. De Nardo, F. Fabozzi,³ C. Gatto, L. Lista, D. Monorchio, P. Paolucci, D. Piccolo,
C. Sciacca

Università di Napoli Federico II, Dipartimento di Scienze Fisiche and INFN, I-80126, Napoli, Italy

M. A. Baak, G. Raven, H. L. Snoek

*NIKHEF, National Institute for Nuclear Physics and High Energy Physics, NL-1009 DB Amsterdam, The
Netherlands*

C. P. Jessop, J. M. LoSecco

University of Notre Dame, Notre Dame, Indiana 46556, USA

T. Allmendinger, G. Benelli, L. A. Corwin, K. K. Gan, K. Honscheid, D. Hufnagel, P. D. Jackson,
H. Kagan, R. Kass, A. M. Rahimi, J. J. Regensburger, R. Ter-Antonyan, Q. K. Wong

Ohio State University, Columbus, Ohio 43210, USA

N. L. Blount, J. Brau, R. Frey, O. Igonkina, J. A. Kolb, M. Lu, R. Rahmat, N. B. Sinev, D. Strom,
J. Strube, E. Torrence

University of Oregon, Eugene, Oregon 97403, USA

²Also with Università della Basilicata, Potenza, Italy

³Also with Università della Basilicata, Potenza, Italy

A. Gaz, M. Margoni, M. Morandin, A. Pompili, M. Posocco, M. Rotondo, F. Simonetto, R. Stroili, C. Voci
Università di Padova, Dipartimento di Fisica and INFN, I-35131 Padova, Italy

M. Benayoun, H. Briand, J. Chauveau, P. David, L. Del Buono, Ch. de la Vaissière, O. Hamon,
B. L. Hartfiel, M. J. J. John, Ph. Leruste, J. Malcès, J. Ocariz, L. Roos, G. Therin
*Laboratoire de Physique Nucléaire et de Hautes Energies, IN2P3/CNRS, Université Pierre et Marie
Curie-Paris6, Université Denis Diderot-Paris7, F-75252 Paris, France*

L. Gladney, J. Panetta
University of Pennsylvania, Philadelphia, Pennsylvania 19104, USA

M. Biasini, R. Covarelli
Università di Perugia, Dipartimento di Fisica and INFN, I-06100 Perugia, Italy

C. Angelini, G. Batignani, S. Bettarini, F. Bucci, G. Calderini, M. Carpinelli, R. Cenci, F. Forti,
M. A. Giorgi, A. Lusiani, G. Marchiori, M. A. Mazur, M. Morganti, N. Neri, E. Paoloni, G. Rizzo,
J. J. Walsh
Università di Pisa, Dipartimento di Fisica, Scuola Normale Superiore and INFN, I-56127 Pisa, Italy

M. Haire, D. Judd, D. E. Wagoner
Prairie View A&M University, Prairie View, Texas 77446, USA

J. Biesiada, N. Danielson, P. Elmer, Y. P. Lau, C. Lu, J. Olsen, A. J. S. Smith, A. V. Telnov
Princeton University, Princeton, New Jersey 08544, USA

F. Bellini, G. Cavoto, A. D'Orazio, D. del Re, E. Di Marco, R. Faccini, F. Ferrarotto, F. Ferroni,
M. Gaspero, L. Li Gioi, M. A. Mazzoni, S. Morganti, G. Piredda, F. Polci, F. Safai Tehrani, C. Voena
Università di Roma La Sapienza, Dipartimento di Fisica and INFN, I-00185 Roma, Italy

M. Ebert, H. Schröder, R. Waldi
Universität Rostock, D-18051 Rostock, Germany

T. Adye, N. De Groot, B. Franek, E. O. Olaiya, F. F. Wilson
Rutherford Appleton Laboratory, Chilton, Didcot, Oxon, OX11 0QX, United Kingdom

R. Aleksan, S. Emery, A. Gaidot, S. F. Ganzhur, G. Hamel de Monchenault, W. Kozanecki, M. Legendre,
G. Vasseur, Ch. Yèche, M. Zito
DSM/Daphnia, CEA/Saclay, F-91191 Gif-sur-Yvette, France

X. R. Chen, H. Liu, W. Park, M. V. Purohit, J. R. Wilson
University of South Carolina, Columbia, South Carolina 29208, USA

M. T. Allen, D. Aston, R. Bartoldus, P. Bechtle, N. Berger, R. Claus, J. P. Coleman, M. R. Convery,
M. Cristinziani, J. C. Dingfelder, J. Dorfan, G. P. Dubois-Felsmann, D. Dujmic, W. Dunwoodie,
R. C. Field, T. Glanzman, S. J. Gowdy, M. T. Graham, P. Grenier,⁴ V. Halyo, C. Hast, T. Hryn'ova,
W. R. Innes, M. H. Kelsey, P. Kim, D. W. G. S. Leith, S. Li, S. Luitz, V. Luth, H. L. Lynch,
D. B. MacFarlane, H. Marsiske, R. Messner, D. R. Muller, C. P. O'Grady, V. E. Ozcan, A. Perazzo,
M. Perl, T. Pulliam, B. N. Ratcliff, A. Roodman, A. A. Salnikov, R. H. Schindler, J. Schwiening,
A. Snyder, J. Stelzer, D. Su, M. K. Sullivan, K. Suzuki, S. K. Swain, J. M. Thompson, J. Va'vra, N. van

⁴Also at Laboratoire de Physique Corpusculaire, Clermont-Ferrand, France

Bakel, M. Weaver, A. J. R. Weinstein, W. J. Wisniewski, M. Wittgen, D. H. Wright, A. K. Yarritu, K. Yi,
C. C. Young

Stanford Linear Accelerator Center, Stanford, California 94309, USA

P. R. Burchat, A. J. Edwards, S. A. Majewski, B. A. Petersen, C. Roat, L. Wilden

Stanford University, Stanford, California 94305-4060, USA

S. Ahmed, M. S. Alam, R. Bula, J. A. Ernst, V. Jain, B. Pan, M. A. Saeed, F. R. Wappler, S. B. Zain

State University of New York, Albany, New York 12222, USA

W. Bugg, M. Krishnamurthy, S. M. Spanier

University of Tennessee, Knoxville, Tennessee 37996, USA

R. Eckmann, J. L. Ritchie, A. Satpathy, C. J. Schilling, R. F. Schwitters

University of Texas at Austin, Austin, Texas 78712, USA

J. M. Izen, X. C. Lou, S. Ye

University of Texas at Dallas, Richardson, Texas 75083, USA

F. Bianchi, F. Gallo, D. Gamba

Università di Torino, Dipartimento di Fisica Sperimentale and INFN, I-10125 Torino, Italy

M. Bomben, L. Bosisio, C. Cartaro, F. Cossutti, G. Della Ricca, S. Dittongo, L. Lanceri, L. Vitale

Università di Trieste, Dipartimento di Fisica and INFN, I-34127 Trieste, Italy

V. Azzolini, N. Lopez-March, F. Martinez-Vidal

IFIC, Universitat de Valencia-CSIC, E-46071 Valencia, Spain

Sw. Banerjee, B. Bhuyan, C. M. Brown, D. Fortin, K. Hamano, R. Kowalewski, I. M. Nugent, J. M. Roney,
R. J. Sobie

University of Victoria, Victoria, British Columbia, Canada V8W 3P6

J. J. Back, P. F. Harrison, T. E. Latham, G. B. Mohanty, M. Pappagallo

Department of Physics, University of Warwick, Coventry CV4 7AL, United Kingdom

H. R. Band, X. Chen, B. Cheng, S. Dasu, M. Datta, K. T. Flood, J. J. Hollar, P. E. Kutter, B. Mellado,
A. Mihalyi, Y. Pan, M. Pierini, R. Prepost, S. L. Wu, Z. Yu

University of Wisconsin, Madison, Wisconsin 53706, USA

H. Neal

Yale University, New Haven, Connecticut 06511, USA

1 INTRODUCTION

The search for lepton flavor violation (LFV) in charged lepton processes is one of the cleanest ways to look for new physics beyond the Standard Model (SM). In the SM with the massless neutrinos, the total lepton number and lepton flavors are conserved, so that processes like $\tau^- \rightarrow \mu^- \eta$ [1] are strictly forbidden. The recent discovery of neutrino oscillations [2] indicates that the neutrinos have a very small and non-zero mass, and the lepton flavor is not conserved in the neutral lepton sector. However, in the simplest extension of the SM, which accommodates the neutrino mass and mixing, the expected branching ratios for lepton flavor violating processes in the charged lepton sector are too small to be experimentally accessible. Thus, any observation of LFV in the charged lepton sector would be an unambiguous signature of new physics beyond the SM [3]. The decay $\tau^- \rightarrow \mu^- \eta$ is of particular interest because it could be enhanced in supersymmetric models [4] due to the potentially large coupling of the Higgs boson to the $s\bar{s}$ pairs and its associated color factors. The most stringent upper limit published to date on this decay is $\mathcal{B}_{UL} < 1.5 \times 10^{-7}$ at 90% confidence level (c.l.) with 154 fb^{-1} of e^+e^- annihilation data collected by the Belle experiment [5].

2 THE *BABAR* DETECTOR AND DATASET

The results presented in this paper are based upon data collected by the *BABAR* detector at the PEP-II storage ring. Details of the detector are described elsewhere [6]. Charged particles are reconstructed as tracks with a 5-layer silicon vertex tracker (SVT) and a 40-layer drift chamber (DCH) inside a 1.5-T solenoidal magnet. An electromagnetic calorimeter (EMC) consisting of 6580 CsI(Tl) crystals is used to identify electrons and photons. A ring-imaging Cherenkov detector (DIRC) is used to identify charged pions and kaons and provides additional electron identification information. The flux return of the solenoid, instrumented with resistive plate chambers (IFR) and limited streamer tubes (LST), is used to identify muons.

The data sample consists of an integrated luminosity of $L = 314.5 \text{ fb}^{-1}$ collected at a center-of-mass (C.M.) energy \sqrt{s} near 10.58 GeV. With an average cross section of $\sigma_{e^+e^- \rightarrow \tau^+\tau^-} = (0.89 \pm 0.02) \text{ nb}$ [7] as determined using the KK2F Monte Carlo (MC) generator [8], this corresponds to a data sample of 279.8×10^6 τ -pair events.

The signal MC is generated with a two-body decay $\tau^- \rightarrow \mu^- \eta$ model, incorporated into the KK2F generator employing the TAUOLA decay package [9]. The potential backgrounds including $e^+e^- \rightarrow \mu^+\mu^-, \tau^+\tau^-, (u\bar{u}, d\bar{d}, s\bar{s})$ mixture, and $c\bar{c}$ processes were studied using the KK2F, EVTGEN [10] & JETSET [11] generators. We also study $b\bar{b}$ Monte Carlo events but find that no events pass our selection criteria. The detector response is modeled using the GEANT4 simulation package [12].

3 ANALYSIS METHOD

3.1 Reconstruction and event selection

We reconstruct the signal process $e^+e^- \rightarrow \tau^+\tau^-$ with one τ^- decaying to $\mu^- \eta$, where $\eta \rightarrow \gamma\gamma$ or $\pi^+\pi^-\pi^0$, using events with zero total charge and with two or four well-reconstructed tracks, where none of the tracks originate from conversion of photons in the material of the detector. The event is divided into hemispheres by the plane perpendicular to the thrust axis [13], which characterizes the direction of maximum energy flow in the event, and is calculated using the energy-momentum information from all the tracks observed in the DCH and energy deposits in the EMC.

For the decay $\tau^- \rightarrow \mu^- \eta$ ($\eta \rightarrow \gamma\gamma$), the signal-side hemisphere is required to contain a pair of energy deposits in the EMC each consistent with being a photon above a 100 MeV energy threshold [14] and only one track (1-prong hemisphere). Extra energy deposits in the EMC greater than the 100 MeV threshold unassociated with any of the identified τ daughters are not allowed in the signal-side hemisphere.

For the 3-prong decay $\tau^- \rightarrow \mu^- \eta$ ($\eta \rightarrow \pi^+ \pi^- \pi^0$), a pair of energy deposits in the EMC each consistent with being a photon above a 50 MeV energy threshold is used to form the π^0 candidate. We then form two possible η candidates by combining the π^0 and the positively charged track with either of the two negatively charged tracks in the signal-side hemisphere. The η candidate closest to its nominal mass ($547.75 \pm 0.12 \text{ MeV}/c^2$ [15]) is assigned to be the true candidate, and the negatively track not associated with the η , is assigned to be the signal muon candidate.

We require all possible η candidates, constructed out of their respective daughters, to have an energy greater than 1.4 GeV and 1.2 GeV for the decay $\eta \rightarrow \gamma\gamma$ and $\eta \rightarrow \pi^+ \pi^- \pi^0$, respectively. We then form the complete τ decay chain, and finally accept an event in either one of the decay modes of η exclusively, based upon the closeness of the signal τ candidate to its nominal mass ($1.777 \text{ GeV}/c^2$ [16]).

For the 1-prong ($\eta \rightarrow \gamma\gamma$) signal candidates, we assign the origin of the two photons from the η to come from the point of closest approach of the signal lepton track to the e^+e^- collision axis. For the 3-prong ($\eta \rightarrow \pi^+ \pi^- \pi^0$) decay, the origin of the photons from the π^0 is taken from the common vertex found by fitting the three tracks in the signal hemisphere.

The respective mass windows for the reconstructed η candidates are:

- $0.515 \text{ GeV}/c^2 < M(\eta \rightarrow \gamma\gamma) < 0.565 \text{ GeV}/c^2$,
- $0.115 \text{ GeV}/c^2 < M(\pi^0 \rightarrow \gamma\gamma) < 0.150 \text{ GeV}/c^2$,
- $0.537 \text{ GeV}/c^2 < M(\eta \rightarrow \pi^+ \pi^- \pi^0) < 0.558 \text{ GeV}/c^2$.

Finally, we kinematically fit for the momentum of the η and the π^0 daughters after applying η and π^0 mass constraints on their respective daughters. We then combine the signal muon track and the η candidates to form τ^- candidates. The signal $\tau^- \rightarrow \mu^- \eta$ decays are identified by two kinematic variables: the beam-energy constrained τ mass (m_{EC}) and $\Delta E = E_\mu + E_\eta - \sqrt{s}/2$, where E_μ and E_η are the energy of the μ and the η candidate in the C.M. frame. These two variables are independent apart from small correlations arising from initial and final state radiation.

The mean and standard deviation of the m_{EC} and ΔE distributions near their statistical maxima for the reconstructed $\tau^- \rightarrow \mu^- \eta$ ($\eta \rightarrow \gamma\gamma$) MC signal events are: $\langle m_{\text{EC}} \rangle = 1777.9 \text{ MeV}/c^2$, $\sigma(m_{\text{EC}}) = 8.25 \text{ MeV}/c^2$, $\langle \Delta E \rangle = -13.4 \text{ MeV}$, $\sigma(\Delta E) = 40.8 \text{ MeV}$, whereas for $\tau^- \rightarrow \mu^- \eta$ ($\eta \rightarrow \pi^+ \pi^- \pi^0$) MC signal events the corresponding quantities are: $\langle m_{\text{EC}} \rangle = 1777.7 \text{ MeV}/c^2$, $\sigma(m_{\text{EC}}) = 5.6 \text{ MeV}/c^2$, $\langle \Delta E \rangle = -7.1 \text{ MeV}$, $\sigma(\Delta E) = 31.0 \text{ MeV}$. The shift from zero in $\langle \Delta E \rangle$ comes from the leakage of the measured photon energy from deposits in the EMC. We do not look at the data events within a $\pm 3\sigma$ rectangular region centered at $(\langle m_{\text{EC}} \rangle, \langle \Delta E \rangle)$ in the m_{EC} vs. ΔE plane, until completing all optimization and systematic studies of the selection criteria.

The τ candidate is considered for further analysis if the signal lepton track is consistent with being identified as a muon, and not an electron or a kaon, using a set of particle identification (PID) criteria using DCH, EMC, DIRC and IFR information, which has a muon identification efficiency of about 85% and 65% inside the polar angle coverages of $[17^\circ, 57^\circ]$ and $[57^\circ, 155^\circ]$, respectively, for tracks with momentum greater than $0.5 \text{ GeV}/c$. This provides the correct association of the

reconstructed particles having the τ as their mother for 99.8% of selected signal MC events inside a $\pm 5\sigma$ rectangular region in m_{EC} vs. ΔE plane for both the decay channels.

To reduce backgrounds from $e^+e^- \rightarrow \mu^+\mu^-$ processes, we require the total C.M. momentum of all the tracks observed in the DCH and unassociated energy deposits in the EMC on the tag-side hemisphere (defined to be the one opposite to the signal-side hemisphere) to be less than 4.75 GeV/c for both the channels.

Other non- τ backgrounds are suppressed by requiring the polar angle of the missing momentum (θ_{miss}) associated with the neutrinos in the event to lie within the detector acceptance ($-0.76 < \cos \theta_{\text{miss}} < 0.92$), and the scaled missing C.M. transverse momentum relative to the beam axis ($p_{\text{miss}}^T/\sqrt{s}$) to be greater than 0.082.

A tag-side hemisphere containing a single track is classified as e-tag, μ -tag or h-tag if the track is exclusively identified as an electron (e-tag), as a muon (μ -tag), or as neither (h-tag) and if the total neutral C.M. energy in the hemisphere is no more than 200 MeV. If the total neutral C.M. energy in the hemisphere is more than 200 MeV and the track is neither an electron nor a muon it is classified as ρ -tag. If the tag-side contains three tracks, the event is classified as a 3h-tag for the $\tau^- \rightarrow \mu^- \eta$ ($\eta \rightarrow \gamma\gamma$) search, whereas for the 3-prong signal decay channel of η we use only 1-prong decays of the τ in the tag-side hemisphere.

We assume that the $\tau^- \rightarrow \mu^- \eta$ decay fully reconstructs the direction of the τ^+ in the hemisphere opposite the signal candidate. We then calculate the invariant mass squared (m_ν^2) of the unobserved particle, assumed to be $\nu(s)$, from the τ^+ decay, assuming that the energy of the τ^+ is given by the beam energy.

A cut of $-1.0 \text{ GeV}^2/c^4 < m_\nu^2 < 2.5 \text{ GeV}^2/c^4$ is applied to the e-tag, μ -tag and h-tag in the search for the $\tau^- \rightarrow \mu^- \eta$ ($\eta \rightarrow \gamma\gamma$) decay. For the ρ -tag, we require $-1.0 \text{ GeV}^2/c^4 < m_\nu^2 < 1.0 \text{ GeV}^2/c^4$ and for the 3h-tag, we require $-0.2 \text{ GeV}^2/c^4 < m_\nu^2 < 1.0 \text{ GeV}^2/c^4$ in the $\eta \rightarrow \gamma\gamma$ decay mode. For $\eta \rightarrow \pi^+\pi^-\pi^0$ mode, we require $-1.25 \text{ GeV}^2/c^4 < m_\nu^2 < 2.5 \text{ GeV}^2/c^4$ for all tags. In addition to the above requirements, we apply cuts on the invariant mass on the tag-side (M_{tag}), calculated from the tracks observed in the DCH and unassociated neutral energy deposits in the EMC, to be less than $0.4 \text{ GeV}/c^2$ for the h-tag and $0.6 \text{ GeV}/c^2 < M_{\text{tag}} < 1.35 \text{ GeV}/c^2$ for the ρ -tag.

The cuts on the different variables have been applied so as to minimize the expected upper limit at 90% c.l. [17] on the branching ratio of the signal $\tau^- \rightarrow \mu^- \eta$ decay, in a background only hypothesis, estimated using Monte Carlo (MC) simulation of background events.

After this selection, 10.08% and 5.43% of the $\tau^- \rightarrow \mu^- \eta$ ($\eta \rightarrow \gamma\gamma$) and $\tau^- \rightarrow \mu^- \eta$ ($\eta \rightarrow \pi^+\pi^-\pi^0$) MC signal events survive within a Grand Signal Box (GSB) region defined as: $m_{\text{EC}} \in [1.5, 2.0] \text{ GeV}/c^2$, $\Delta E \in [-0.8, 0.4] \text{ GeV}$. The data distribution of m_{EC} and ΔE inside the GSB is plotted as dots in Figure 1. About 70% of the selected signal MC events inside the GSB lie within a $\pm 2\sigma$ rectangular region in the m_{EC} vs. ΔE plane. These MC events are shown by the shaded region in Figure 1.

3.2 Background estimation

The GSB regions excluding the $\pm 3\sigma$ blinded region contain 65 and 23 data events, while the luminosity-normalized sum of the MC backgrounds yield (74.6 ± 9.0) and (34.3 ± 5.2) events for the 2 channels respectively. For the $\tau^- \rightarrow \mu^- \eta$ ($\eta \rightarrow \gamma\gamma$) channel, 24%, 62% and 9% of the MC background events have a true μ only, a true η candidate only and both true μ and true η candidates, respectively. For the $\tau^- \rightarrow \mu^- \eta$ ($\eta \rightarrow \pi^+\pi^-\pi^0$) channel, 4%, 37% and 4% of the MC background events have a true μ only, a true η candidate only and both true μ and true η

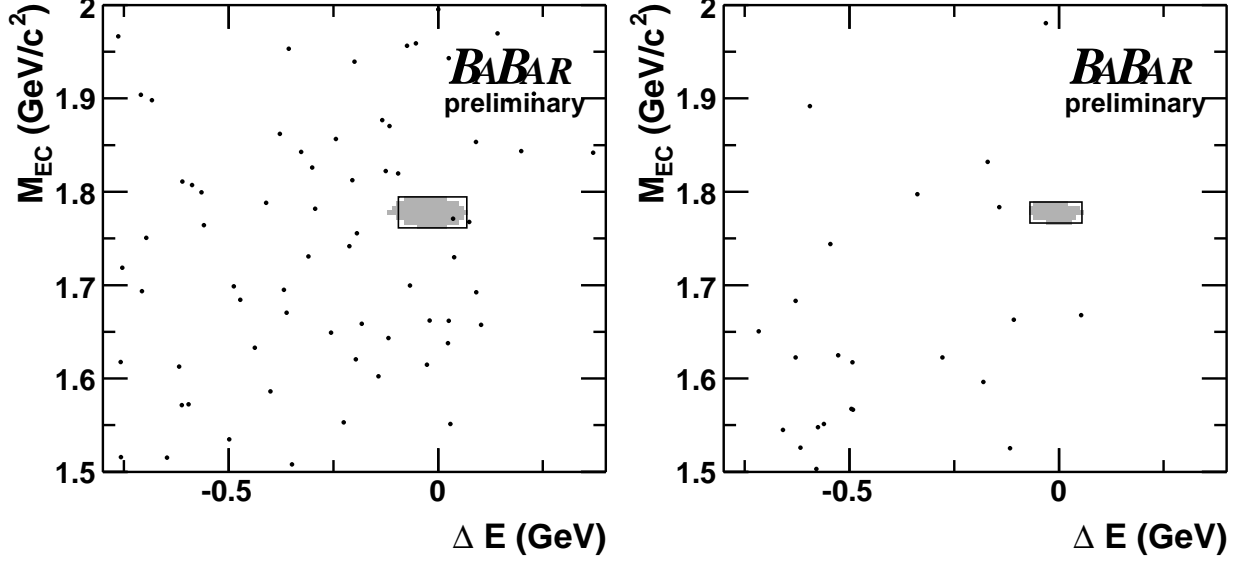


Figure 1: The ΔE and m_{EC} distributions for the data (shown as dots) after all the selection criteria have been applied, in the search for the $\tau^- \rightarrow \mu^- \eta$ ($\eta \rightarrow \gamma\gamma$) decay (left) and the $\tau^- \rightarrow \mu^- \eta$ ($\eta \rightarrow \pi^+ \pi^- \pi^0$) decay (right). The shaded region contains 70% of the selected signal MC events inside the Grand Signal Box for both modes. The $\pm 2\sigma$ signal box is also overlaid.

candidates, respectively. The major source of backgrounds come from either a mis-identification of a pion track as a muon candidate or the in-efficiency in η and π^0 reconstruction.

The number of expected backgrounds in the signal box is extracted from an un-binned maximum likelihood fit to the distributions of the m_{EC} and ΔE variables for the data events inside the non-blinded parts of the GSB region, while the shape of the distributions have been obtained from MC. The number of background events ($N_{2\sigma}^{\text{data}}$) inside the $\pm 2\sigma$ signal box is estimated as:

$$N_{2\sigma}^{\text{data}} = \frac{\int_{2\sigma} PDF_{\text{tot}}}{\int_{\text{GSB}-3\sigma} PDF_{\text{tot}}} \times N_{\text{GSB}-3\sigma}^{\text{data}}$$

where $\int_{2\sigma} PDF_{\text{tot}}$ and $\int_{\text{GSB}-3\sigma} PDF_{\text{tot}}$ are the probability density functions (PDFs) integrated over the the signal box and the non-blinded parts of the GSB regions, $N_{\text{GSB}-3\sigma}^{\text{data}}$ are the number of data events in the non-blinded parts of the GSB region, and the PDF_{tot} is defined as:

$$PDF_{\text{tot}} = (f_{\mu} \times PDF_{\mu}) + (f_{\tau} \times PDF_{\tau}) + ([1 - f_{\mu} - f_{\tau}] \times PDF_{uds})$$

where the f_{μ} and f_{τ} are the fractions of $\mu^+ \mu^-$ and $\tau^+ \tau^-$ background contributions. The PDF_{μ} , PDF_{τ} and PDF_{uds} are non-parametric PDFs [18] obtained from the respective background MC events after applying the same final selection criteria. The corresponding projections of the PDFs obtained from MC for the individual components and the total fit to the data in the GSB region excluding the $\pm 3\sigma$ blinded region for m_{EC} and ΔE variables are shown in Figure 2, along with the data points. The $\pm 2\sigma$ signal box is indicated by hatches.

The number of background events from the fit to the data in the non-blinded parts of the GSB region for $\tau^- \rightarrow \mu^- \eta$ ($\eta \rightarrow \gamma\gamma$) and $\tau^- \rightarrow \mu^- \eta$ ($\eta \rightarrow \pi^+ \pi^- \pi^0$) searches are (0.64 ± 0.08)

and (0.07 ± 0.02) events, respectively. The observed and the expected number of background events inside the neighbouring boxes in the non-blinded parts of the GSB are shown in Table 1 and Table 2 for the respective channels.

As a cross-check, we also estimate the background assuming a uniform distribution over the GSB in m_{EC} vs. ΔE plane. This simple interpolation gives the number of backgrounds in signal box to be (0.60 ± 0.07) and (0.10 ± 0.02) for $\tau^- \rightarrow \mu^- \eta$ ($\eta \rightarrow \gamma\gamma$) and $\tau^- \rightarrow \mu^- \eta$ ($\eta \rightarrow \pi^+ \pi^- \pi^0$), respectively.

$\tau^- \rightarrow \mu^- \eta$ ($\eta \rightarrow \gamma\gamma$)	$(5 - 3)\sigma$	$(7 - 5)\sigma$	$(9 - 7)\sigma$	$(11 - 9)\sigma$	$(11 - 3)\sigma$
# of observed events	4	3	5	7	19
# of expected events	2.5 ± 0.3	3.7 ± 0.5	4.8 ± 0.6	5.7 ± 0.7	16.7 ± 2.1

Table 1: The number of observed and expected data events inside the $5\sigma - 3\sigma$, $7\sigma - 5\sigma$, $9\sigma - 7\sigma$, $11\sigma - 9\sigma$ and $11\sigma - 3\sigma$ neighboring boxes in the m_{EC} vs. ΔE for the search for the decay $\tau^- \rightarrow \mu^- \eta$ ($\eta \rightarrow \gamma\gamma$).

$\tau^- \rightarrow \mu^- \eta$ ($\eta \rightarrow \pi^+ \pi^- \pi^0$)	$(5 - 3)\sigma$	$(7 - 5)\sigma$	$(9 - 7)\sigma$	$(11 - 9)\sigma$	$(11 - 3)\sigma$
# of observed events	1	0	0	2	3
# of expected events	0.3 ± 0.1	0.4 ± 0.1	0.5 ± 0.1	0.7 ± 0.1	1.9 ± 0.4

Table 2: The number of observed and expected data events inside the $5\sigma - 3\sigma$, $7\sigma - 5\sigma$, $9\sigma - 7\sigma$, $11\sigma - 9\sigma$ and $11\sigma - 3\sigma$ neighboring boxes in the m_{EC} vs. ΔE plane for the search for the decay $\tau^- \rightarrow \mu^- \eta$ ($\eta \rightarrow \pi^+ \pi^- \pi^0$).

4 SYSTEMATIC STUDIES

Table 3 is a summary of the relative systematic uncertainties in the signal efficiency estimation. The largest systematic uncertainties are due to the signal track momentum and the photon energy scale and resolution, which are the tracking and calorimetry errors introduced by applying the final cut on the $\pm 2\sigma$ signal region. In order to assess the systematic errors associated with these scale and resolution uncertainties, the peak and resolution of m_{EC} as well as the ΔE are varied. The errors associated with the modeling of each election variable is estimated from the relative change in signal efficiency when varying the cut by the Data-MC difference in the mean of that variable.

Other sources of systematic uncertainties include those arising from trigger and filter efficiencies, tracking and neutral energy reconstruction efficiencies, the PID error associated with signal muon track identification, beam energy scale and spread, luminosity estimation and cross-section of the $e^+e^- \rightarrow \tau^+\tau^-$ process.

As we use 2.3 million MC signal events, the contribution to the uncertainty arising from signal MC statistics is negligible.

All contributions to the systematic uncertainties are added in quadrature to give a total relative systematic uncertainty of 7.5% and 8.6% for the $\tau^- \rightarrow \mu^- \eta$ ($\eta \rightarrow \gamma\gamma$) and the $\tau^- \rightarrow \mu^- \eta$ ($\eta \rightarrow \pi^+ \pi^- \pi^0$) channels respectively.

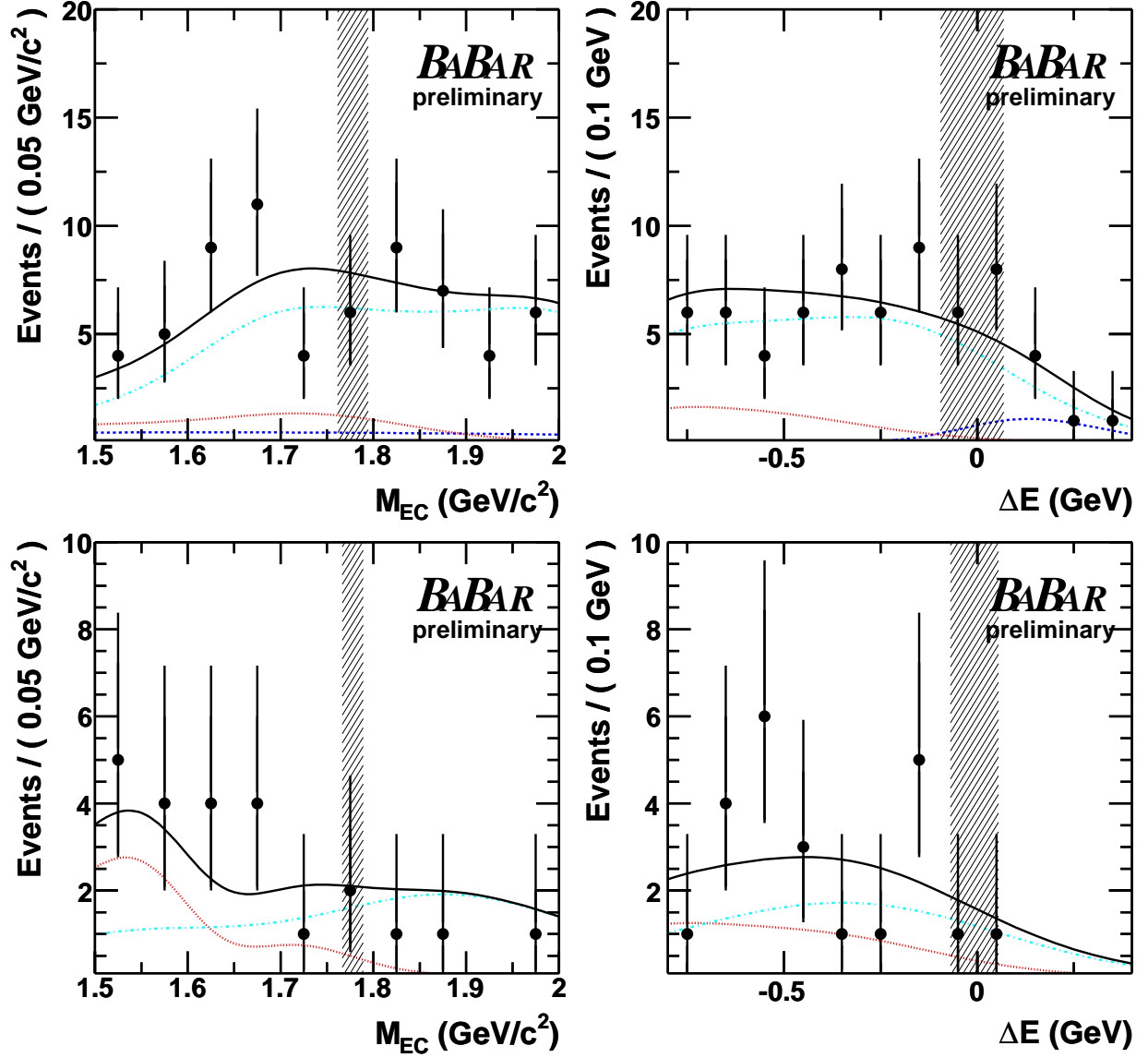


Figure 2: The fit to the data distributions of m_{EC} and ΔE variables in the GSB regions excluding the $\pm 3\sigma$ blinded region in the search for the $\tau^- \rightarrow \mu^- \eta$ ($\eta \rightarrow \gamma\gamma$) decay (top row) and for the $\tau^- \rightarrow \mu^- \eta$ ($\eta \rightarrow \pi^+ \pi^- \pi^0$) decay (bottom row) are shown along with the data distributions (as dots) and the background MC components ($\mu^+ \mu^-$ in dashed, $\tau^+ \tau^-$ in dotted and uds in dashed-dotted). The shaded region is the $\pm 2\sigma$ signal box for both modes.

The dominant contribution to the uncertainty of background estimation arises from the statistical error on the number of data events surviving the final selection inside the non-blinded parts of the GSB, and from the variation of the fitted f_μ and f_τ within $\pm 1\sigma$ from the fit to the data. A small contribution of 1.9% and 0.9% on the relative uncertainties from a bias in the fit arising from blinding of the $\pm 3\sigma$ rectangular region in the m_{EC} vs. ΔE plane during estimation of PDFs from the MC background samples has been included in the above-mentioned estimate.

Uncertainty ($\delta\varepsilon/\varepsilon$)	%	%
	($\eta \rightarrow \gamma\gamma$)	($\eta \rightarrow \pi^+\pi^-\pi^0$)
Trigger and filter efficiency	1.0	0.4
Tracking efficiency	1.3	2.2
Neutral energy reconstruction efficiency	3.3	3.3
PID error associated with signal muon track	3.0	2.7
Modeling of the selection variables	3.9	3.4
Signal track and photon energy scale and resolution	3.7	5.8
Beam energy scale and spread	0.4	0.5
Luminosity and $\tau^+\tau^-$ production cross-section	2.3	2.3
Total	7.5	8.6

Table 3: Summary of the relative systematic uncertainties (in %) of the signal efficiency for both decay modes $\tau^- \rightarrow \mu^-\eta$ ($\eta \rightarrow \gamma\gamma$) and $\tau^- \rightarrow \mu^-\eta$ ($\eta \rightarrow \pi^+\pi^-\pi^0$).

5 RESULTS

The upper limit of $\tau^- \rightarrow \mu^-\eta$ is calculated using $\mathcal{B}_{UL}^{90} = N_{UL}^{90}/(2L\sigma_{\tau\tau}\mathcal{B}\varepsilon)$, where N_{UL}^{90} is the 90% c.l. upper limit on the number of signal events expected within the $\pm 2\sigma$ box in m_{EC} vs. ΔE plane, ε is the reconstruction efficiency and \mathcal{B} is the branching ratio of the η decay modes under consideration.

To obtain a combined upper limit, we add the signal efficiencies for the individual channels weighted by their respective branching ratios using the formula:

$$\mathcal{B}\varepsilon = (\mathcal{B}_1 \times \varepsilon_1 + \mathcal{B}_2 \times \varepsilon_2)$$

where $\varepsilon_1 = (7.03 \pm 0.53)\%$, $\varepsilon_2 = (3.67 \pm 0.32)\%$ are the signal reconstruction efficiencies for the two decay modes $\tau^- \rightarrow \mu^-\eta$ ($\eta \rightarrow \gamma\gamma$) and $\tau^- \rightarrow \mu^-\eta$ ($\eta \rightarrow \pi^+\pi^-\pi^0$), and \mathcal{B}_1 , \mathcal{B}_2 are the branching ratios of $\eta \rightarrow \gamma\gamma$ and $\eta \rightarrow \pi^+\pi^-\pi^0$ ($\pi^0 \rightarrow \gamma\gamma$), respectively. Thus, for the decay modes combined, taking into account the errors from similar sources as correlated, we have a combined efficiency for reconstructing $\tau^- \rightarrow \mu^-\eta$ of $\mathcal{B}\varepsilon = (3.59 \pm 0.41)\%$. This corresponds to a 11.4% relative systematic uncertainty on the total selection efficiency.

We sum the backgrounds inside the $\pm 2\sigma$ signal box from the above two channels to obtain a background expectation of (0.71 ± 0.08) events for the combined upper limit calculation. Inside the $\pm 2\sigma$ signal box, we observe only one event in the search for the decay $\tau^- \rightarrow \mu^-\eta$ ($\eta \rightarrow \gamma\gamma$), and none in the search of the decay $\tau^- \rightarrow \mu^-\eta$ ($\eta \rightarrow \pi^+\pi^-\pi^0$).

The limit is calculated including all uncertainties using the technique of Cousins and Highland [19] following the implementation of Barlow [20]. In this technique, MC samples are generated according to a Poisson distribution with mean $(s + b)$ where the background, b , and signal, s , are each drawn randomly from Gaussian distributions describing their respective PDFs. The values of the mean and standard deviation for the background Gaussian are 0.71 and 0.08 events, respectively. The mean of the signal Gaussian is $(2L\sigma_{\tau\tau}\mathcal{B}_{UL}\varepsilon)$ and the standard deviation is the error on $(2L\sigma_{\tau\tau}\mathcal{B}_{UL}\varepsilon)$. The branching ratio, \mathcal{B}_{UL} , is varied until we find a value for which 10% of the sample yields a number of events less than the one event observed in the data. At 90% c.l. this procedure gives an observed upper limit for $\mathcal{B}(\tau^- \rightarrow \mu^-\eta)$ to be 1.6×10^{-7} including effects

of systematic uncertainties on the signal efficiency and background estimation for both the decay modes combined. Averaging the number of observed events along with its poisson fluctuation, the expected upper limit for $\mathcal{B}(\tau^- \rightarrow \mu^- \eta)$ at 90% c.l. is 1.4×10^{-7} .

The η branching ratio, the selection efficiency, the number of expected and observed background events and the observed upper limit at 90% c.l. with the systematic uncertainties are shown in Table 4 for the two modes separately and combined.

Decay modes	Branching Ratio of η (%)	Efficiency (%)	Background events		Upper Limit (@90% c.l.)
			Expected	Observed	
$\tau^- \rightarrow \mu^- \eta$ ($\eta \rightarrow \gamma\gamma$)	39.42 ± 0.26	7.03 ± 0.53	0.64 ± 0.08	1	2.1×10^{-7}
$\tau^- \rightarrow \mu^- \eta$ ($\eta \rightarrow \pi^+ \pi^- \pi^0$)	22.32 ± 0.40	3.67 ± 0.32	0.07 ± 0.02	0	4.9×10^{-7}
$\tau^- \rightarrow \mu^- \eta$	3.59 ± 0.41		0.71 ± 0.08	1	1.6×10^{-7}

Table 4: The η branching ratio, the selection efficiency, the number of expected and observed background events and the observed upper limit for the two modes separately and combined with systematic uncertainty.

6 SUMMARY

The search for the SM forbidden decay $\tau^- \rightarrow \mu^- \eta$ is performed using 314.5 fb^{-1} data. We find one event consistent with the signal signature for an expected background of (0.71 ± 0.08) events. A 90% c.l. upper limit on the branching ratio is calculated to be 1.6×10^{-7} including effects of systematic uncertainties on the signal efficiency and background estimation.

7 ACKNOWLEDGMENTS

We are grateful for the extraordinary contributions of our PEP-II colleagues in achieving the excellent luminosity and machine conditions that have made this work possible. The success of this project also relies critically on the expertise and dedication of the computing organizations that support *BABAR*. The collaborating institutions wish to thank SLAC for its support and the kind hospitality extended to them. This work is supported by the US Department of Energy and National Science Foundation, the Natural Sciences and Engineering Research Council (Canada), Institute of High Energy Physics (China), the Commissariat à l’Energie Atomique and Institut National de Physique Nucléaire et de Physique des Particules (France), the Bundesministerium für Bildung und Forschung and Deutsche Forschungsgemeinschaft (Germany), the Istituto Nazionale di Fisica Nucleare (Italy), the Foundation for Fundamental Research on Matter (The Netherlands), the Research Council of Norway, the Ministry of Science and Technology of the Russian Federation, and the Particle Physics and Astronomy Research Council (United Kingdom). Individuals have received support from the Marie-Curie IEF program (European Union) and the A. P. Sloan Foundation.

References

- [1] Charge conjugate mode for all the decays are implied throughout this paper unless otherwise stated.
- [2] B. T. Cleveland *et al.*, *Astrophys. J.* **496**, 505 (1998); Y. Fukuda *et al.* [Super-Kamiokande Collab.], *Phys. Rev. Lett.* **81**, 1562 (1998); Q. R. Ahmad *et al.* [SNO Collab.], *Phys. Rev. Lett.* **89**, 011301 (2002); M. H. Ahn *et al.* [K2K Collab.], *Phys. Rev. Lett.* **90**, 041801 (2003); K. Eguchi *et al.* [KamLAND Collab.], *Phys. Rev. Lett.* **90**, 021802 (2003).
- [3] E. Ma, *Nucl. Phys. Proc. Suppl.* **123**, 125 (2003).
- [4] M. Sher *et al.*, *Phys. Rev.* **D66**, 057301 (2002).
- [5] Y. Enari *et al.* (Belle Collaboration), *Phys. Lett.* **B622**, 218 (2005).
- [6] B. Aubert *et al.* (BABAR Collaboration), *Nucl. Instrum. Methods Phys. Res., Sect. A* **479**, 1 (2002).
- [7] The uncertainty was conservatively estimated by comparisons of the cross section between the generators KK2F [8] and KORALB: S. Jadach and Z. Was, *Comput. Phys. Commun.* **85**, 453 (1995).
- [8] B. F. Ward, S. Jadach, and Z. Was, *Nucl. Phys. Proc. Suppl.* **116**, 73 (2003).
- [9] S. Jadach, Z. Was, R. Decker, and J. H. Kuhn, *Comput. Phys. Commun.* **76**, 361 (1993).
- [10] D. J. Lange, *Nucl. Instrum. Methods Phys. Res., Sect. A* **462**, 152 (2001).
- [11] T. Sjöstrand, *Comput. Phys. Commun.* **82**, 74 (1994).
- [12] S. Agostinelli *et al.* (GEANT4 Collaboration), *Nucl. Instrum. Methods Phys. Res., Sect. A* **506**, 250 (2003).
- [13] S. Brandt *et al.*, *Phys. Lett.* **12** 57 (1964); E. Fahri, *Phys. Rev. Lett.* **39** 1587 (1977).
- [14] All measured quantities are quoted in the laboratory frame, unless otherwise mentioned.
- [15] S. Eidelman *et al.* *Phys. Lett. B* **592**, 1 (2004).
- [16] J. Z. Bai *et al.* (BES Collaboration), *Phys. Rev. D* **53**, 20 (1996).
- [17] G. J. Feldman and R. D. Cousins, *Phys. Rev. D* **57**, 3873 (1998).
- [18] K. Cranmer, *Comput. Phys. Commun.* **136**, 198 (2001).
- [19] R. D. Cousins and V. L. Highland, *Nucl. Instrum. Methods Phys. Res., Sect. A* **320**, 331 (1992).
- [20] R. Barlow, *Comput. Phys. Comm.* **149**, 97 (2002).